Cell Metabolism, ***Volume 10***

Supplemental Data

Translation Attenuation through eIF2α Phosphorylation Prevents Oxidative Stress and Maintains the Differentiated State in β Cells

Sung Hoon Back, Donalyn Scheuner, Jaeseok Han, Benbo Song, Mark Ribick, Junying Wang, Robert D. Gildersleeve, Subramaniam Pennathur, and Randal J. Kaufman

Supplemental Results

Pancreatic β-Cell-Specific Expression of Wild-Type (WT) eIF2α Rescues β Cell Loss in Homozygous *eIF2α A/A* Mutant Mice

Previous studies of mice having an alanine mutation at the Ser51 phosphorylation site in eIF2α demonstrated that eIF2α phosphorylation is required for differentiation and/or maintenance of pancreatic beta cells at an embryonic stage and to prevent hypoglycemia in neonates (Scheuner et al., 2001). Three primary questions arise regarding the phenotype of these mice. First, is the beta cell deficiency in these mice caused by an absence of eIF2α phosphorylation in the beta cell or is it due to an absence of this signal in another cell type that influences beta cell function? Second, why do beta cells fail in the absence of eIF2α phosphorylation? Finally, what is the relationship between beta cell failure and the neonatal lethal phenotype observed in homozygous *A/A* mice? To address these questions, transgenic mice that express wild-type (wt) eIF2α specifically in beta cells were derived (Figures S1A-S1D). Beta cell-specific wt *eIF2α* transgene (*β-Tg*) expression restored beta cell mass and ultrastructure in homozygous *A/A* embryos (Figures S1E-S1G), indicating that the beta cell death associated with Ser51Ala mutation is due to a lack of eIF2α phosphorylation in the beta cell. However, beta cell-specific wt eIF2α expression did not prevent the postnatal lethality (Table S1), suggesting neonatal viability requires eIF2α phosphorylation in cell types additional to the beta cell.

ATF4 Is Not Required for β Cell Function

To examine the role of ATF4 in beta cells, we evaluated glucose homeostasis islet morphology, and pancreatic cell death in *Atf4*-null mice. Although most homozygous *Atf4*-null mice die during embryonic, postnatal, or neonatal stages (Hettmann et al., 2000), the blood glucose levels and GTTs measured in a limited number of wild-type (wt) and homozygous *Atf4*-null mice were not significantly different when they were fed either standard chow or challenged with a high-fat (HF) diet for 9 weeks (Figures S9A, S9B, and data not shown). Although morphological analysis and insulin and glucagon immunofluorescence revealed that the islets of *Atf4*-null mice appeared normal (Figures S9C and S9D), there was severe exocrine pancreas atrophy and a high frequency of apoptotic exocrine cells in sections of *Atf4*-null mice (Figure S9E). These experiments show that ATF4 is not required to preserve beta cell function, suggesting that decreased *Atf4* mRNA translation due to defective eIF2α phosphorylation in *fTg*-deleted *A/A;fTg/0;CreER/0* mutant mice is unlikely a cause for the beta cell failure.

Supplemental Discussion

Our finding that eIF2α phosphorylation is required for function and survival of differentiated beta cells contrasts with observations from analysis of beta cell-specific *Perk*-deletion that led to the proposal that PERK is not required to maintain function of differentiated beta cells (Zhang et al., 2006). There are several possible reasons that may account for the different observations. First, in contrast to deletions of any single eIF2α kinase gene, it is possible that the homozygous *A/A* mutation has a more dramatic phenotype due to the absence of basal eIF2α phosphorylation and constitutive attenuation of protein synthesis. Second, it is possible that cells adapt to PERK deficiency by compensatory mechanisms. Where *Perk*-deletion caused abnormal proinsulin accumulation in the ER in neonatal mice, proinsulin localization was normalized at 30 days after birth (see Zhang et al., *Cell Metab*, 2006, 4, 491-497, Figures 4H and 4I) (Zhang et al., 2006). In contrast, we observed that abnormal proinsulin ER localization became more severe with time after beta cell-specific deletion of the *fTg* in *A/A;fTg/0;CreER/0* mice. This suggests that a compensatory pathway, possibly mediated by increased signaling through alternative eIF2α kinases, may restore function to *Perk*-deleted beta cells. Indeed, studies suggest that GCN2 and PKR may phosphorylate eIF2α in response to ER stress (Hamanaka et al., 2005; Jiang et al., 2004; Onuki et al., 2004; Srivastava et al., 1995). These compensatory eIF2α kinase signaling pathways would not be effective in beta cells from Tam-treated *A/A;fTg/0;CreER/0* mice because their primary substrate for phosphorylation is absent. Finally, recent studies demonstrate repopulation of beta cell mass can occur after massive beta cell destruction (Cano et al., 2008; Nir et al., 2007). Since Zhang et al. (Zhang et al., 2006) utilized mice with two floxed *Perk* alleles, it is possible that islet mass is repopulated with cells that do not harbor deletion of both floxed *Perk* alleles. Since the *A/A;fTg/0;CreER/0* mice we have studied have a single copy of the *eIF2α fTg*, a single recombination event will generate eIF2α phosphorylation-deficient cells. Direct analysis of deletion efficiency and eIF2α phosphorylation in the islets of *Perk*-deleted adult mice should provide insight into the potential for recovery of cells that activate compensatory eIF2α phosphorylation pathways or escape complete *Perk* deletion. In our analysis it was possible to directly detect transgene-deleted cells by expression of EGFP. Our findings that show a selective loss of the EGFP-positive beta cells occurs in *A/A;fTg/0;CreER/0* mice upon deletion of the *eIF2α fTg* convincingly demonstrate that eIF2α phosphorylation is required for beta cell function and/or survival.

The strain differences are another possible reason for the different observations (Berglund et al., 2008; Clee and Attie, 2007; Mathews et al., 2004; Zraika et al., 2006). Beta cell specific *Perk*-deleted (*βPKO*) mice were derived from *Perk*-null (*PKO*) mice in either C57BL6/6J or 129SvEvTac backgrounds or mixtures of both. Our experiments were performed in *A/A;fTg/0;CreER/0* mice with a C57BL/6J, SJL, and CD-1 background (See Animal breeding schemes in Supplemental Experimental Procedures). It is possible that genetic background(s) in *A/A;fTg/0;CreER/0* mice may contribute susceptibility for beta cell death by modulating accumulation of misfolded proteins in the ER lumen, controlling ROS production, and/or altering cell death signaling mechanisms. It is also possible that genetic trait(s) responsible for ER stress- and ROS-mediated beta cell death may be removed or diluted by our multiple breeding scheme to generate *A/A;fTg/0;CreER/0* mice. To date, it is unknown how mouse genetic background may contribute to ER stress-mediated beta cell death.

Supplemental Experimental Procedures

Construction of a β-Cell-Specific *eIF2α* Transgene Vector *(β-Tg)* and Characterization of *β-Tg* Copy Number and Expression Level in Transgenic Mice

The 0.9 kb murine wt *eIF2α* cDNA was inserted into the RIP vector (a gift of Dr. Richard D. Palmiter, University of Washington) containing the rat *Insulin II* promoter (RIP) and intron, along with the mouse major histocompatibility complex *Eα II* polyadenylation sequence (pA) (Figure S1A) (D'Alessio et al., 1994).

The transgenic construct *(β-Tg)* was microinjected into C57BL/6JxSJL fertilized embryos and they were implanted into pseudopregnant females. Transgenic founder mice (*S/S;β-Tg/0*) were identified by PCR-based genotyping of tail DNA with the primer pair (*Ins-β-Tg*) described in Table S4. Three transgenic founders (*S/S;β-Tg/0*) were isolated. One transgenic founder 3* was chosen for detailed Southern blot analysis of genomic DNA for *β-Tg* copy number (Figure S1B) and quantitative RT-PCR measurement of the total *eIF2α* mRNA level from isolated islets (Figure S1C). The beta cell-specific expression of *eIF2α* mRNA driven from *β-Tg* was also confirmed by semi-quantitative RT-PCR analysis in isolated tissues from transgenic founder 3***** (Figure S1D).

Construction of a Floxed *eIF2α* Transgene Containing Vector (*fTg*) and Characterization of *fTg* Copy Number and Expression Level in Transgenic Mice

The 0.9 kb murine wt *eIF2α* cDNA was inserted into between SalI and XmaI site of pDNR-CMV plasmid (CLONTECH) to generate pDNR-CMV-LoxP-eIF2α which has one *loxP* site in front of the *eIF2α* cDNA. To generate pCMV-LoxP-eIF2α-LoxP that is flanked by *loxP* sites, the NotI fragment from pDNR-CMV was inserted into the XmaI site of pDNR-CMV-LoxP-eIF2α. To generate pCMV-LoxP-eIF2α-LoxP-EGFP, the NotI and SalI fragment of pCMV-LoxP-eIF2α-LoxP was then inserted into pEGFP-N1 to position the *EGFP* sequence downstream of the *eIF2α* cDNA. The 2 kb NotI fragment (LoxP-eIF2α-LoxP-EGFP) from pCMV-LoxP-eIF2α-LoxP-EGFP was inserted into pCX-EGFP digested with EcoRI to generate pCX-LoxP-eIF2α-LoxP-EGFP.

A 4.4 kb floxed *eIF2α* fragment (*fTg*) from pCX-LoxP-eIF2α-LoxP-EGFP was released by SspI and SfiI restriction enzyme digestion, purified by gel fractionation, and microinjected into C57BL/6JxSJL fertilized embryos utilizing standard procedures. Injected embryos were implanted into pseudopregnant females. Transgenic founder mice (*S/S;fTg/0*) were identified by PCR-based genotyping of tail DNA with three primer sets (Enh-Pro, eIF2α-EGFP, and EGFP) described in Table S4. Southern blot (Figure S2A) and Northern blot analyses (Figures S2C and S2D) of 21 PCR positive-transgenic founders led to the selection of one transgenic founder (Figure S2A, Founder 11* and Figure S2C transgenic mouse 7*). Founder 11* (*S/S;fTg/0*) has a single copy of the transgene (*LoxP-eIF2α-LoxP-EGFP*), determined by Southern blot analysis (Figure S2B). The expression of floxed *eIF2α fTg* mRNA was confirmed by Northern blot analysis of multiple tissues (Figure S2D). The level of wt eIF2α protein derived from floxed *eIF2α fTg* mRNA in islets was confirmed by Western blot analysis using rabbit anti-eIF2α antibody (Cell Signaling Technology) and mouse anti-α-Tubulin antibody (Sigma), and quantified by the Scion image program (Scion Corporation) (Figures S2E and F)

Southern and Northern Blot Analysis

Southern and Northern blot analyses were performed as previously described. (Back et al., 2006; Lee et al., 2002). ^{32}P-labeled probes were prepared using a random prime labeling system (Amersham Pharmacia). Southern blot analysis was performed with a probe derived from either a 1 kb BglII fragment containing the *eIF2*α cDNA from the beta cell-specific targeting vector β-*Tg* (Figure S1B) or a 0.8 kb PCR product containing the *EGFP* cDNA from pCX-LoxP-eIF2α-LoxP-EGFP vector (Figures S2A and S2B). The PCR product was amplified with Forward primer: 5'-GTCGACCGGTCGCCACCA-3' and Reverse primer: 5'-AGATCTCAGTGGTATTTG-3'. Band intensities were quantified by phosphorimaging. Northern blot analysis was performed using probes derived from either a 0.7 kb XmnI-XmaI fragment containing the *eIF2*α cDNA from the pCX-LoxP-eIF2α-LoxP-EGFP vector (Figure S2C) or the same *EGFP* cDNA used for Southern Blotting (Figure S2D).

Animal Breeding Schemes

eIF2*α β*-Tg* (*β-Tg/0*) *Mice. A transgenic founder 3* (*S/S;β-Tg/0,* mixed background of C57BL/6J and SJL) was backcrossed to heterozygous *S/A* (backcrossed onto a C57Bl/6J background for more than 10 generations) mice to produce *S/A;β-Tg/0* strains that were bred with *S/A* mice to generate experimental progeny: *S/S;0/0*, *S/S;β-Tg/0*, *S/A;0/0, S/A;β-Tg/0, A/A*;*0/0*, and *A/A;β-Tg/0*.

eIF2*α *fTg* (*fTg/0*) *Mice. A transgenic founder 11* (*S/S;fTg/0*, mixed background of C57BL/6J and SJL) was bred with heterozygous *S/A* (backcrossed onto a C57BL/6J background for more than 10 generations) mice to obtain *S/A;fTg/0* mice. Secondly, *S/A;fTg/0* mice were crossed with heterozygous *S/A* mice to obtain *A/A;fTg/0* progeny. *A/A;fTg/0* mice were interbred to maintain the strain. *S/A;CreER/0 mice* (mixed background of C57BL/6J and CD-1) were generated by breeding heterozygous *S/A* mice with *CreER/0* mice (mixed background of C57BL/6J and CD-1). *A/A;fTg/0* mice were crossed with *S/A;CreER/0* mice (heterozygous *S/A* mice carrying Cre recombinase) to produce progeny for experiments: *S/A;0/0;0/0*, *S/A;0/0;CreER/0, S/A;fTg/0;0/0*, *S/A;fTg/0;CreER/0, A/A;0/0;0/0*, *A/A;0/0;CreER/0, A/A;fTg/0;0/0*, *A/A;fTg/0;CreER/0*. Genotypes of the mice were identified by PCR-based genotyping of tail DNA with the primer pairs described in Table S4.

Measurements of Protein Synthesis

Islets were washed two times in Kreb's Ringer-bicarbonate buffer (115 mM NaCl, 5mM KCl, 10 mM $NaHCO_3$, 2.5 mM $MgCl_2$, 2.5 mM $CaCl_2$, and 20 mM HEPES [pH 7.4], 0.1% BSA) containing 2.8 mM glucose and preincubated in the same buffer 1 hr at 37 °C. Centrifugation was performed and islets were exchanged into incubation buffer (2.8 or 16.7 mM glucose) for 1 hr at 37 °C. During the last 20 min of incubation, 50 μCi [^{35}S] methionine (Met) and cysteine (Cys) (TRAN^{35}S-LABEL^{TM}, MP Biomedical, Inc.) was added. Metabolic labeling was terminated with ice-cold Kreb's buffer containing unlabeled Met (0.6 mg/ml) and Cys (0.96 mg/ml) and two further washes were performed. The islet pellets were lysed in 50 μl of lysis buffer (50 mM Tris-Cl [pH 8.0], 150 mM NaCl, 1% NP-40, 1% SDS, and protease inhibitors), sonicated at 4 °C for 15 min, and cleared by centrifugation at 12,000*g* for 10 min at 4 °C. Three aliquots of 5 μl each were taken for measurement of total protein synthesis by trichloroacetic acid (TCA) precipitation on Whatman filter paper. Duplicate aliquots of 5 μl each from the remainder of the radiolabeled lysate were assayed for total protein concentration by Bio-Rad *DC* protein assay kit.

Proinsulin synthesis was measured by immunoprecipitation of 50 μg of whole lysate protein per sample with 5 μg of mouse anti-proinsulin antibody (HyTest Ltd.). Immunoprecipitated proteins were resolved on a 10% Bis-Tris acrylamide gel (Criterion^{TM} XT precast gel, Bio-Rad). The incorporation of [^{35}S] Met or Cys into proinsulin was quantified by phosphorimaging.

Atf 4 Null Mice and HF Diet Study

Atf4 (Creb-2)-null mice were a gift from Dr. Jeffrey M. Leiden (Hettmann et al., 2000). *Atf4*$^{+/+}$ and *Atf4*$^{-/-}$ mice at 8-10 weeks of age were housed pair-wise and fed a 45% HF diet (Research Diets Inc. D12451) for up to 9 weeks.

Cell Culture

Wild-type *S/S* and homozygous *A/A* immortalized hepatocytes were cultured as described previously. (Sakaki et al., 2008)

Statistical Analysis

All data are presented as means ± SEM. Statistical significance of difference between groups was evaluated using a Student t-test or ANOVA one-way test (Tukey's test). $P < 0.05$ was considered significant. *$P < 0.05$, **$P < 0.01$, ***$P < 0.001$.

All other procedures for Supplemental Experimental Procedures are described in EXPERIMENTAL PROCEDURES of main text.

Table S1. Survival ratio of neonatal progeny (n=75) from breeding of *S/A;β-Tg/0* X *S/A* mice

Genotype	*S/S*	*S/A*	*A/A*
β-Tg (-)	10/75 (0.13)	20/75 (0.27)	4(dead*)/75 (0.05)
β-Tg (+)	8/75 (0.11)	23/75 (0.31)	10 (dead*)/75 (0.13)
Expected frequency	**0.125**	**0.25**	**0.125**

The pups (dead*) were dead within 24 hr after birth

Table S2. Survival ratio of young progeny (1~2 months old) from breeding of *A/A;fTg/0* X *S/A* mice

Genotype:	*S/A*	*S/A:fTg/0*	*A/A*	*A/A:fTg/0*
Observed:	45/139 (0.32)	49/139 (0.35)	N.D	45/139 (0.32)
Expected frequency:	**0.33**	**0.33**	**(all dead)**	**0.33**

N.D : not detected

Table S3. Body mass of young progeny (1 month old) from breeding of *A/A;fTg/0* X *S/A* mice

Genotype:	*S/A*	*S/A:fTg/0*	*A/A*	*A/A:fTg/0*
Male (g):	19.6±0.60 (n=6)	18.6±0.78 (n=18)	N.D	18.6±0.03 (n=18)
Female (g):	15.6±0.35 (n=6)	16.2±0.25 (n=18)	N.D	14.8±0.50 (n=16)

N.D : not detected

Table 4. PCR primers

Gene name	5' oligonucleotide	3' oligonucleotide	Usage
18S rRNA	CGCTTCCTTACCTGGTTGAT	GAGCGACCAAAGGAACCATA	q-PCR
beta actin	GATCTGGCACCACACACCTTCT	GGGGTGTTGAAGGTCTCAAA	q-PCR
A20	TGGTTCCAATTTTGCTCCTT	CGTTGATCAGGTGAGTCGTG	q-PCR
Atf4	ATGGCCGGCTATGGATGAT	CGAAGTCAAACTCTTTCAGATCCATT	q-PCR
Bak	CCTGAAACCTTGGCCCCT	AGCCGTGCAAAGACGAAGAC	q-PCR
Bax	GGAGCAGCTTGGGAGCG	AAAAGGCCCCTGTCTTCATGA	q-PCR
Bcl2	ACTTCGCAGAGATGTCCAGTCA	TGGCAAAGCGTCCCCTC	q-PCR
Bcl-xl	GTAAACTGGGGTCGCATTGT	TGGATCCAAGGCTCTAGGTG	q-PCR
Beta2	GCAAACTGAAAATCAAAACCAA	GGATTGTTATCAAAAGTTGAAAGATG	q-PCR
Bim	GGAGATACGGATTGCACAGGAG	CCTTCTCCATACCAGACGGAAG	q-PCR
BiP	GGTGCAGCAGGACATCAAGTT	CCCACCTCCAATATCAACTTGA	q-PCR
Catalase (Cat)	ACCCTCTTATACCAGTTGGC	GCATGCACATGGGGCCATCA	q-PCR
Cebpα	TGGACAAGAACAGCAACGAG	TCACTGGTCAACTCCAGCAC	q-PCR
Chop	CTGCCTTTCACCTTGGAGAC	CGTTTCCTGGGGATGAGATA	q-PCR
Dr5	ATAAAAAGAGGCTGTGAACGGG	GGTCCAAGAGAGACGA	q-PCR
Edem1	GCAATGAAGGAGAAGGAGACCC	TAGAAGGCGTGTAGGCAGATGG	q-PCR
Erdj4	GAATTAATCCTGGCCTCCAA	CAGGGTGGTACTTCATGGCT	q-PCR
Ero1α	GCATTGAAGAAGGTGAGCAA	ATCATGCTTGGTCCACTGAA	q-PCR
Ero1β	GGGCCAAGTCATTAAAGGAA	TTTATCGCACCCAACACAGT	q-PCR
Erp72	AGTCAAGGTGGTGGTGGGAAAG	TGGGAGCAAAATAGATGGTAGGG	q-PCR
Fas	AACCAGACTTCTACTGCGATTCTCC	CCTTTTCCAGCACTTTCTTTTCCG	q-PCR
Fkbp11	ACACGCTCCACATACACTACACGG	ATGACTGCTCTTCGCTTCTCTCCC	q-PCR
Gadd34	CCCGAGATTCCTCTAAAAGC	CCAGACAGCAAGGAAATGG	q-PCR
Glucagon (Gcg)	AAACCAAGATCACTGACAAGAAATAGGT	TTTGAAATTGTACATCCCAAGTGAC	q-PCR
Glut2	CAATTACCGACAGCCCATCC	TCCTGAGAACTGCTGGGCC	q-PCR
Gpx1	ACAGTCCACCGTGTATGCCTTC	CTCTTCATTCTTGCCATTCTCCTG	q-PCR
Gpx2	GAAAGACAAGCTGCCCTACC	TCCATATGATGAGCTTGGGA	q-PCR
Grp94	AATAGAAAGAATGCTTCGCC	TCTTCAGGCTCTTCTTCTGG	q-PCR
Ho1	CCACACAGCACTATGTAAAGCGTC	GTTCGGGAAGGTAAAAAAAGCC	q-PCR
Herpud1	AGCAGCCGGACAACTCTAAT	CTTGGAAAGTCTGCTGGACA	q-PCR
Herpud2	CCAACAATGTGGACGCTAAC	CTTCACCTGCATCTTCTCCA	q-PCR
Hrd1	TGGCTTTGAGTACGCCATTCT	CCACGGAGTGCAGCACATAC	q-PCR
Iapp	CCTCATCCTCTCTGTGGCAC	CACGTTGGTTGGTGGGAG	q-PCR
Ins1	GCAAGCAGGTCATTGTTTCAAC	AAGCCTGGGTGGGTTTGG	q-PCR
Ins2	TTTGTCAAGCAGCACCTTTG	GGTCTGAAGGTCACCTGCTC	q-PCR
MafA	GCTGGTATCCATGTCCGTGC	GTCGGATGACCTCCTCCTTG	q-PCR
Ngn3	GTCGTTACCCTTCCCCCAAG	CTAGGGCTTTCCGGTTCACA	q-PCR
Noxa	CGCCAGTGAACCCAACG	TTATGTCCGGTGCACTCCAC	q-PCR
p21	CGAGAACGGTGGAACTTTGAC	TCCCAGACGAAGTTGCCCT	q-PCR
p53	AAAACCACTTGATGGAGAGTATTTCA	GCTCCCGGAACATCTCGAA	q-PCR
p58^{IPK}	TCCTGGTGGACCTGCAGTACG	CTGCGAGTAATTTCTTCCCC	q-PCR
Pdx1	GAGCGTTCCAATACGGACCA	TCAGCCGTTCTGTTTCTGGG	q-PCR
Pgc1α	AACCACACCCACAGGATCAGA	TCTTCGCTTTATTGCTCCATGA	q-PCR
Pgc1β	CTTGCTAACATCACAGAGGATATCTTG	GGCAGGTTCAACCCCGA	q-PCR
Pparα	ACGATGCTGTCCTCCTTGATG	GTGTGATAAAGCCATTGCCGT	q-PCR
Pparγ	AGTGGAGACCGCCCAGG	GCAGCAGGTTGTCTTGGATGT	q-PCR
Pdi	CAAGATCAAGCCCCACCTGAT	AGTTCGCCCCAACCAGTACTT	q-PCR
Sod1	GGCCCGGCGGATGA	CGTCCTTTCCAGCAGTCACA	q-PCR
Sod2	GGGTTGGCTTGGTTTCAATAAGGAA	AGGTAGTAAGCGTGCTCCCACACAT	q-PCR
Tnfα	CCCTCACACTCAGATCATCTTCT	GCTACGACGTGGGCTACAG	q-PCR
Tnfr1	CATCCCCAAGCAAGAGTCATG	GCTACAGACGTTCACGATGC	q-PCR
Trb3	TCTCCTCCGCAAGGAACCT	TCTCAACCAGGGATGCAAGAG	q-PCR
Ubc7	TCCTCCAGAAGGAATCGTG	AAGTGGGAAACTCAGGATGG	q-PCR
Ucp2	TACCAGAGCACTGTCGAAGCC	AGTCCCTTTCCAGAGGCCC	q-PCR
Wars	CCTTGGACTACACAGCCAGGA	CTAGGACCGAGGCCTGCAG	q-PCR
Wfs	GTAGCAAGTGGCCCGTCTTC	TGCAGTTGAGGCAGCTGATG	q-PCR
Xbp1-spliced	GAGTCCGCAGCAGGTG	GTGTCAGAGTCCATGGGA	q-PCR
Xbp1-total	AAGAACACGCTTGGGAATGG	ACTCCCCTTGGCCTCCAC	q-PCR
Total eIF2α	CCTGGATACGGTGCCTACG	TGTGGGGTCAAACGCCTATT	q-PCR for endogenous *eIF2α + fTg*
Endo eIF2α	ACTTCGGGATTCACACATCC	GCCAATTCGGATCAGTTTGT	q-PCR for endogenous *eIF2α*
eIF2α transgene	GCTGGTTGTTGTGCTGTCTC	CCACCTCAGGAAATTTGTGTT	q-PCR for *fTg*
β-Tg	GAAACCATCAGCAAGCAGGT	GCCAATTCGGATCAGTTTGT	RT-PCR for *β-Tg*
eIF2α(S51A)	CACACACCCATTCCATGATAGTAATG	CAATGTTGTAGACCCTGACAATGAAGG	Genotyping for *S/A* mutant allele
Ins-β-Tg	CCAGCCCTAAGTGACCAGCTAC	GCCAATTCGGATCAGTTTGT	Genotyping for *β-Tg*
Enh-Pro	CGACATTGATTATTGACTAG	GTAATAGCGATGACTAATAC	Genotyping for *fTg*
eIF2α-EGFP	TGGTTATGAAGGCATTGATG	GCGGACTTGAAGAAGTCGTG	Genotyping for *fTg*
EGFP	TATATCATGGCCGACAAGCA	GAACTCCAGCAGGACCATGT	Genotyping for *fTg*
CRE	GCGGTCTGGCAGTAAAAACTATC	GTGAAACAGCATTGCTGTCACTT	Genotyping for CreER
CREB-2 (WT)	GCAGCAGTGTTGCTGTAACGGAC	CTGGCCAAGCCATCATCCATAGC	Genotyping for *Atf4* wt allele
CREB-2 (Null)	TTTGAGTTGTGCGCTCGGGTGTC	GCTACCGGTGGATGTGGAATGT	Genotyping for *Atf4* null allele

Figure S1

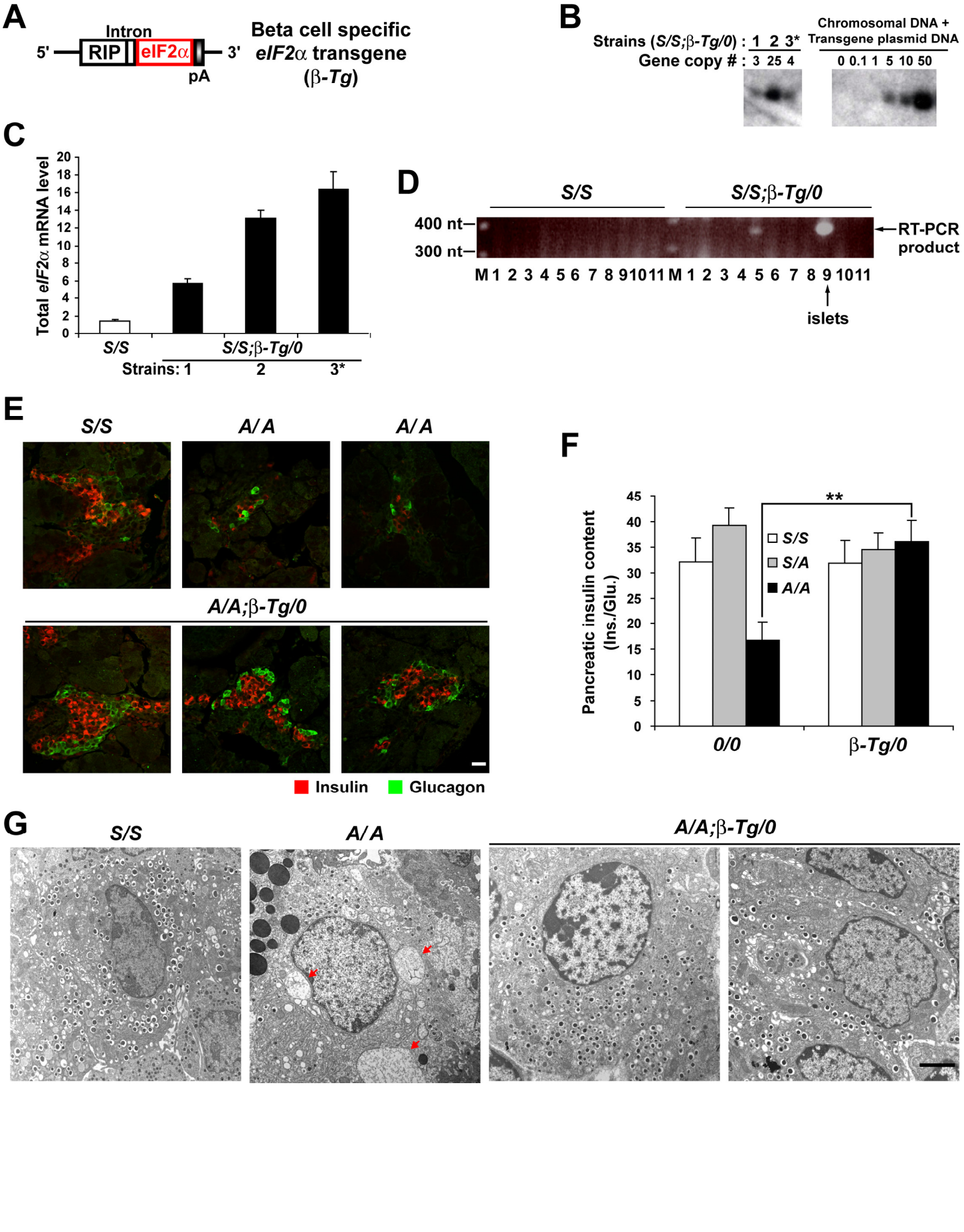
A
Intron
5'
RIP
eIF2α
3'
pA
Beta cell specific
eIF2α transgene
(β-Tg)
B
Strains (S/S;β-Tg/0) : 1 2 3*
Gene copy # : 3 25 4
Chromosomal DNA +
Transgene plasmid DNA
0 0.1 1 5 10 50
C
Total eIF2α mRNA level
20
18
16
14
12
10
8
6
4
2
0
S/S
S/S;β-Tg/0
Strains: 1
2
3*
D
S/S
S/S;β-Tg/0
400 nt
300 nt
RT-PCR
product
M 1 2 3 4 5 6 7 8 9 10 11 M 1 2 3 4 5 6 7 8 9 10 11
islets
E
S/S
A/A
A/A
A/A;β-Tg/0
Insulin
Glucagon
F
Pancreatic insulin content
(Ins./Glu.)
45
40
35
30
25
20
15
10
5
0
**
S/S
S/A
A/A
0/0
β-Tg/0
G
S/S
A/A
A/A;β-Tg/0

Figure S1. β-Cell-Specific Expression of Wild-Type (WT) *eIF2α* (*β-Tg*) Prevents β Cell Loss and Restores Islet Morphology and β Cell Ultrastructure in Homozygous *eIF2α A/A* Embryos

(A) Diagram depicts the structure of the wt *eIF2α* transgene (*β-Tg*) for expression in pancreatic beta cells. RIP and pA represent the rat *insulin II* promoter and the mouse major histocompatibility complex *Eα II* polyadenylation sequence, respectively.
(B) BglII-digested genomic DNA from three different transgenic founders (*S/S:β-Tg/0*) was analyzed by Southern blotting using *eIF2α* cDNA as a hybridization probe. Estimation of transgene copy number was performed by comparison of band intensities with 0-50 copies of *β-Tg* plasmid DNA. The progeny of founder 3* were utilized in further experiments (Figures S1C-S1G).
(C) Total *eIF2α* mRNA levels in isolated islets of progeny from three different transgenic founders were compared to wt control mice at 12 wks of age. Total *eIF2α* mRNA levels were measured by quantitative real-time PCR analysis with a primer pair (Total eIF2α) that recognizes both endogenous and transgene-derived *eIF2α* mRNA. n=3 per group.
(D) Expression of *β-Tg* in multiple tissues was analyzed by semi-quantitative RT-PCR. Total RNA was extracted from different organs, 1-brain, 2-brown fat tissue, 3-heart, 4-intestine, 5-kidney, 6-liver, 7-lung, 8-muscle, 9-pancreatic islets, 10-spleen, 11-white fat tissue, of wt (*S/S*) and a transgenic mouse (*S/S;β-Tg/0*) and RT-PCR was performed with primers *(β-Tg*) spanning the 5' intron of *β-Tg* (Figure S1A).
(E) Insulin and glucagon immunolabeling was performed to visualize islet morphology in pancreas tissue sections obtained from E18.5 embryos. Representative fluorescence images are shown. The scale bar represents 20 μM.
(F) The *β-Tg* transgene rescues insulin content in pancreata from homozygous *A/A* mutant embryos. Measurements of pancreatic insulin content (Ins) were normalized to glucagon (Glu). n= 4-19 E18.5 embryos per group.
(G) Representative transmission electron micrographs from pancreatic sections of E18.5 embryos are shown. Arrows indicate regions of severe ER distention. The scale bars represents 2 μm.
Data are Mean ± SEM, (C) and (E).

Figure S2

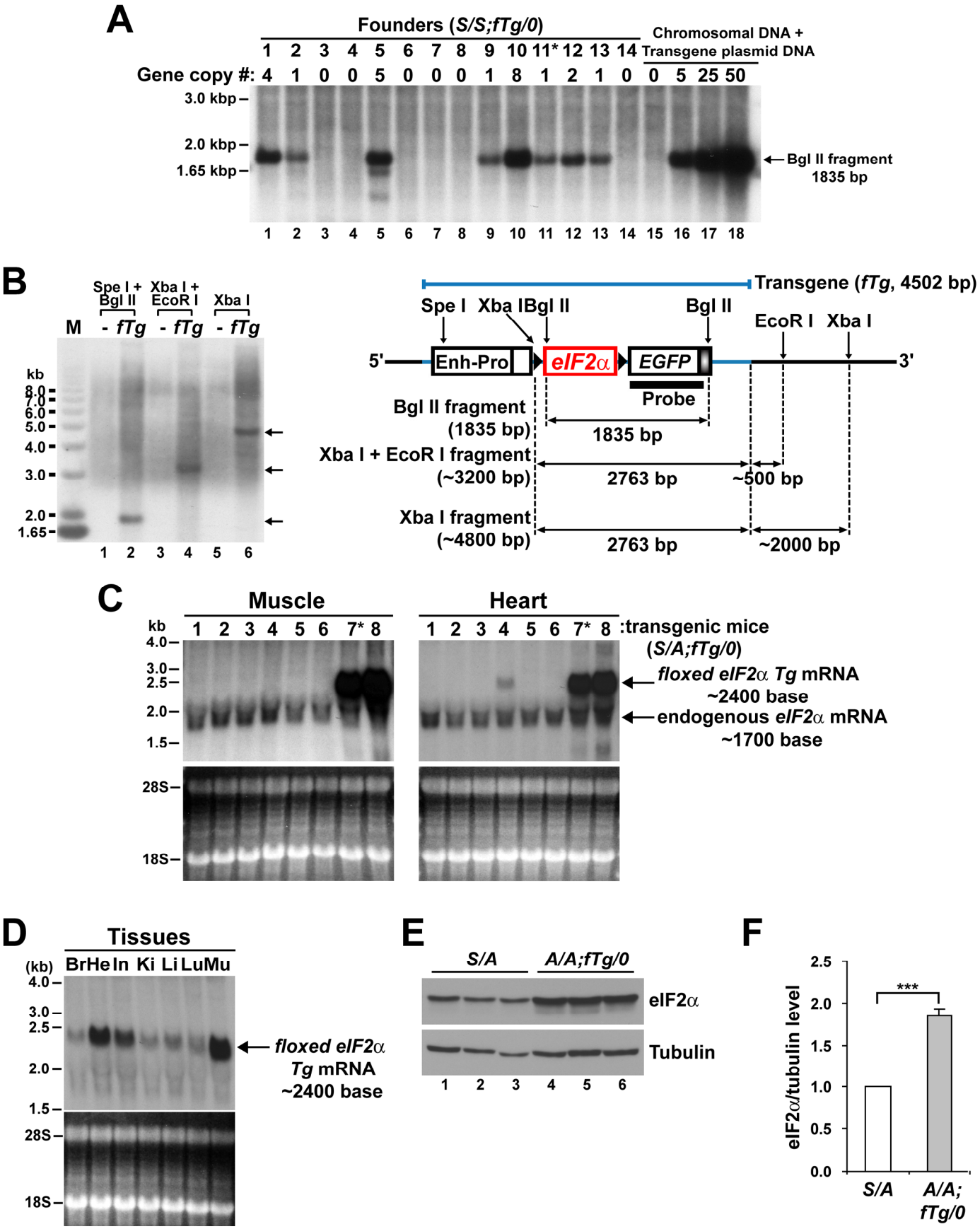
A
Founders (S/S;fTg/0)
1 2 3 4 5 6 7 8 9 10 11* 12 13 14
Chromosomal DNA + Transgene plasmid DNA
Gene copy #: 4 1 0 0 5 0 0 0 1 8 1 2 1 0 0 5 25 50
3.0 kbp
2.0 kbp
1.65 kbp
Bgl II fragment 1835 bp
1 2 3 4 5 6 7 8 9 10 11 12 13 14 15 16 17 18
B
Spe I + Bgl II
Xba I + EcoR I
Xba I
M - fTg - fTg - fTg
kb
8.0
7.0
6.0
5.0
4.0
3.0
2.0
1.65
1 2 3 4 5 6
Transgene (fTg, 4502 bp)
Spe I Xba I Bgl II Bgl II EcoR I Xba I
5'
Enh-Pro
eIF2α
EGFP
3'
Probe
Bgl II fragment (1835 bp)
1835 bp
Xba I + EcoR I fragment (~3200 bp)
2763 bp
~500 bp
Xba I fragment (~4800 bp)
2763 bp
~2000 bp
C
Muscle
Heart
kb
1 2 3 4 5 6 7* 8
1 2 3 4 5 6 7* 8
:transgenic mice (S/A;fTg/0)
4.0
3.0
2.5
2.0
1.5
floxed eIF2α Tg mRNA ~2400 base
endogenous eIF2α mRNA ~1700 base
28S
18S
D
Tissues
(kb)
Br He In Ki Li Lu Mu
4.0
3.0
2.5
2.0
1.5
28S
18S
floxed eIF2α Tg mRNA ~2400 base
E
S/A
A/A;fTg/0
eIF2α
Tubulin
1 2 3 4 5 6
F
eIF2α/tubulin level
2.5
2.0
1.5
1.0
0.5
0.0
***
S/A
A/A; fTg/0

Figure S2. Identification of a Floxed WT *eIF2α fTg* Founder Line that Ubiquitously Expresses *fTg* mRNA from a Single-Copy Transgene

(A) Southern blot analysis of BglII-digested genomic DNA from different transgenic founders (*S/S;fTg/0*) was performed using *EGFP* cDNA as a hybridization probe. Transgene copy number was determined by comparison of band intensities to 0-50 copies of *fTg* plasmid DNA. Progeny from founder 11***** with a single copy *fTg* were utilized in further experiments.
(B) Transgene copy number was determined by Southern blot hybridization of genomic DNA. Three different combinations of restriction endonucleases were used to digest genomic DNA from *S/A* (lanes 1, 3, and 5) and *S/A;fTg/0* mice (lanes 2, 4, and 6). Southern blotting was performed using *EGFP* cDNA as a probe. A transgene XbaI restriction site and chromosomal restriction sites for EcoRI and XbaI that are 3' to the *fTg* integration site combine to yield single fragments of 3.2 and 4.8kb that affirm single site integration.
(C and D) Northern blot analysis (upper panels) detects *fTg* mRNA in muscle and heart tissues from founder animals (*S/A;fTg/0*) (C) and in multiple tissues (D) using *eIF2α* cDNA (C) or *EGFP* cDNA (D) as hybridization probes, respectively. Animal No. 7***** (D) is progeny of Founder No. 11***** in Figure S2A and was the source of total RNA isolated from various organs at 12 wks of age. Tissues are defined as: Brain (Br), Heart (He), Intestine (In), Kidney (Ki), Liver (Li), Lung (Lu), and Muscle (Mu). Ethidium bromide staining (lower panels) is shown as a control for loading and integrity of RNA samples.
(E and F) The expression of wt eIF2α protein derived from *floxed eIF2α fTg* was measured by Western blot analysis comparing islet extracts from *A/A;fTg/0* mice and *S/A* mice.

Figure S3

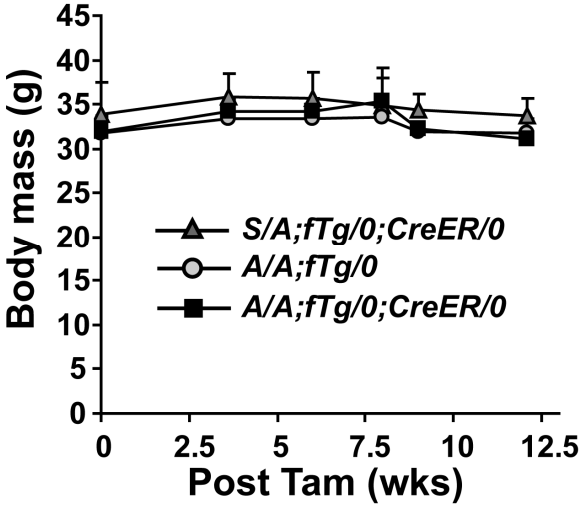

Figure S3. Body Mass Measurements for Transgene (*fTg*)-Deleted *A/A;fTg/0;CreER/0* Mice

At the indicated weeks after Tam injection, body mass measurements were performed in mice fasted for 5-6 hrs. n=5-6 mice per group. Data are Mean ± SEM.

Figure S4

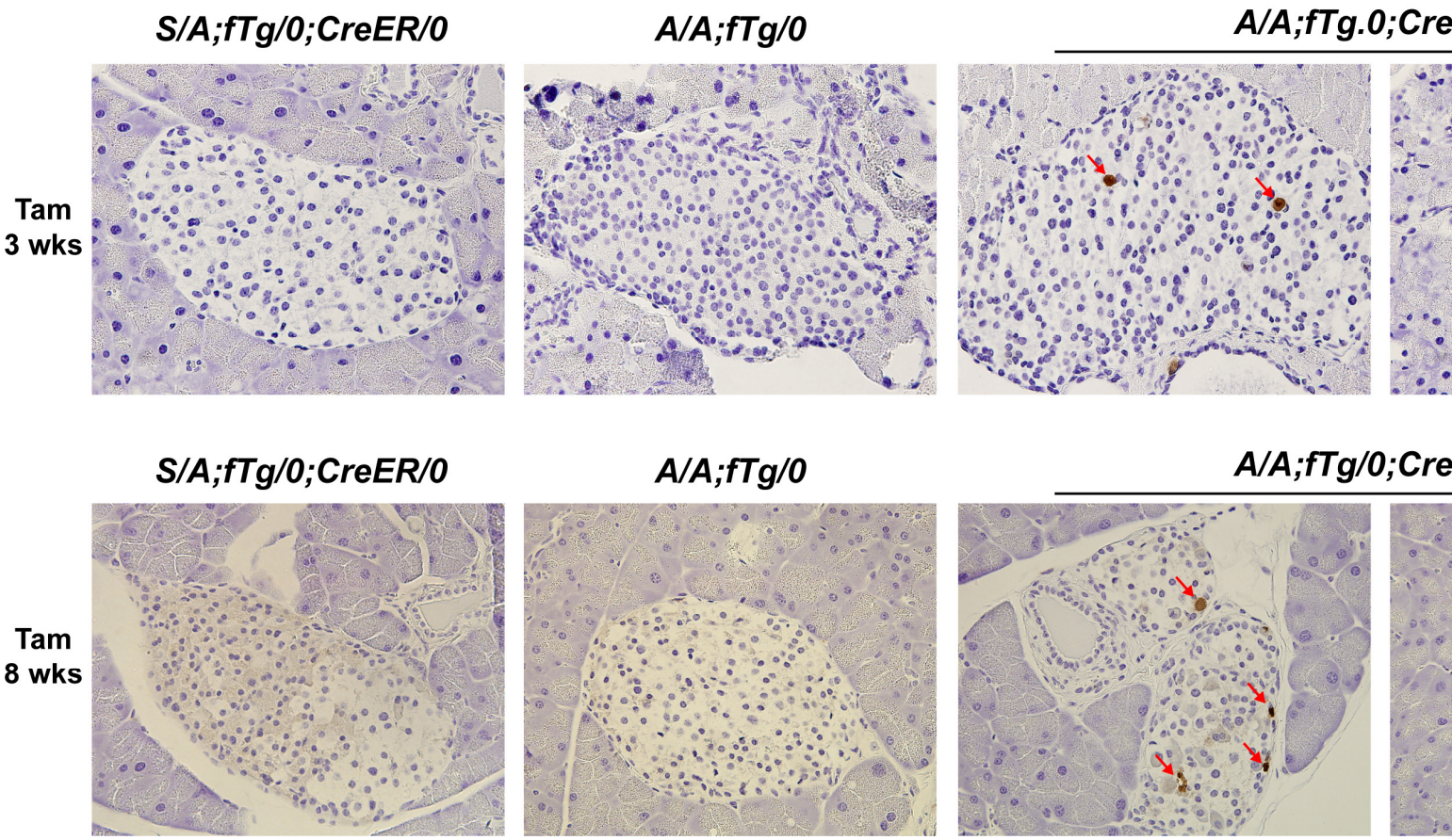

Figure S4. β-Cell-Specific Deletion of WT *eIF2α fTg* Causes β Cell Death

TUNEL staining was performed on sections of pancreata harvested at 3 and 8 wks after Tam injection. n = 5-7 mice per group. The scale bars represent 50 μm.

Figure S5

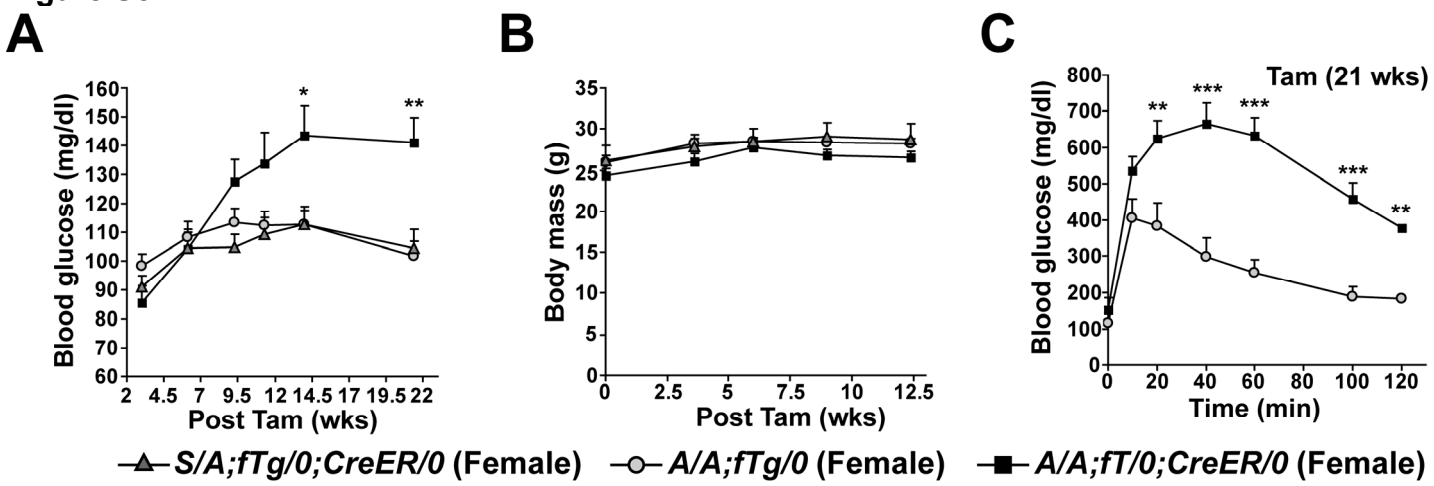

Figure S5. Deletion of *fTg* in β Cells of *A/A;fTg/0;CreER/0* Female Mice Causes Mild Hyperglycemia and Glucose Intolerance

(A and B) At the indicated weeks after tamoxifen injection, blood glucose (A) and body weight (B) measurements were performed in female mice fasted for 5-6 hrs. n=5-7 mice per group.
(C) Glucose tolerance tests were performed 21 wks after tamoxifen administration. n=8-9 mice per group.
Significant differences between *A/A;fTg/0* versus *A/A;fTg/0;CreER/0* mice are indicated.
Data are Mean ± SEM, (A-C).

Figure S6

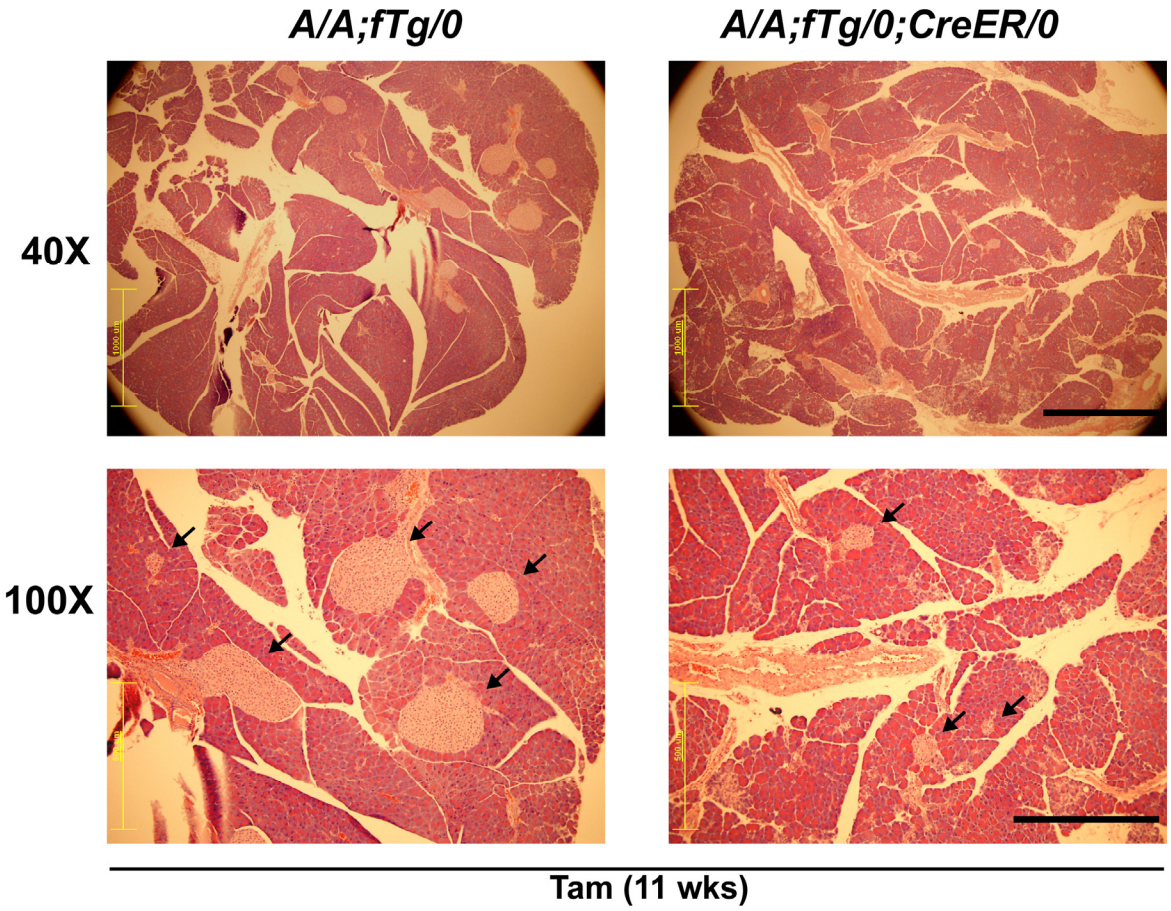

Figure S6. Deletion of *fTg* in β Cells of *A/A;fTg/0;CreER/0* Mice Causes Islet Hypoplasia

Representative images of hematoxylin and eosin (H&E) stained pancreatic tissue sections from *A/A;fTg/0* and *A/A;fTg/0;CreER/0* male mice at 11 wks after tamoxifen treatment are shown. The arrows indicate islets. The scale bar represents 1000 μm in upper panels and 500 μm in lower panels.

Figure S7

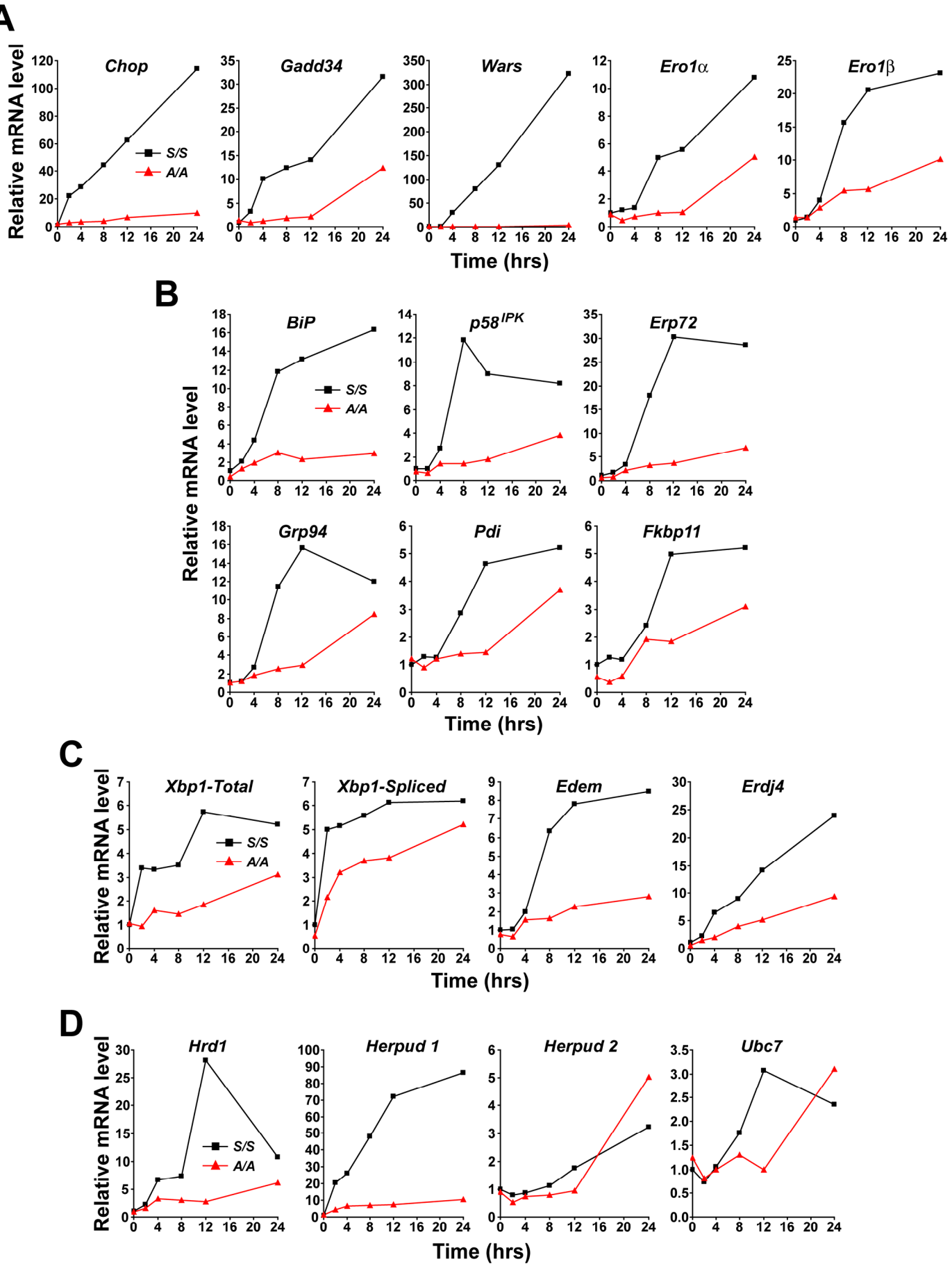
A
Chop
Gadd34
Wars
Ero1α
Ero1β
S/S
A/A
Relative mRNA level
Time (hrs)
B
BiP
p58IPK
Erp72
Grp94
Pdi
Fkbp11
Relative mRNA level
Time (hrs)
C
Xbp1-Total
Xbp1-Spliced
Edem
Erdj4
Relative mRNA level
Time (hrs)
D
Hrd1
Herpud 1
Herpud 2
Ubc7
Relative mRNA level
Time (hrs)

Figure S7. Induction of Many UPR Genes Is Impaired in *eIF2α A/A* Hepatocytes

Total RNA was isolated from *S/S* and *A/A* hepatocytes incubated for 0-24 hrs in the absence or presence of tunicamycin (Tm, 1 μg/ml) and was analyzed by quantitative RT-PCR. Expression values of mRNA were normalized to *beta actin* mRNA levels and expressed as fold induction versus *S/S* hepatocytes without tuncamycin (0 hr).

(A) Genes regulated through eIF2α phosphorylation.

(B) Genes encoding ER chaperone functions.

(C) Genes regulated through the IRE1α/XBP1 pathway.

(D) Genes encoding ERAD machinery.

Data are Mean ± SEM, (A-D).

Figure S8AB

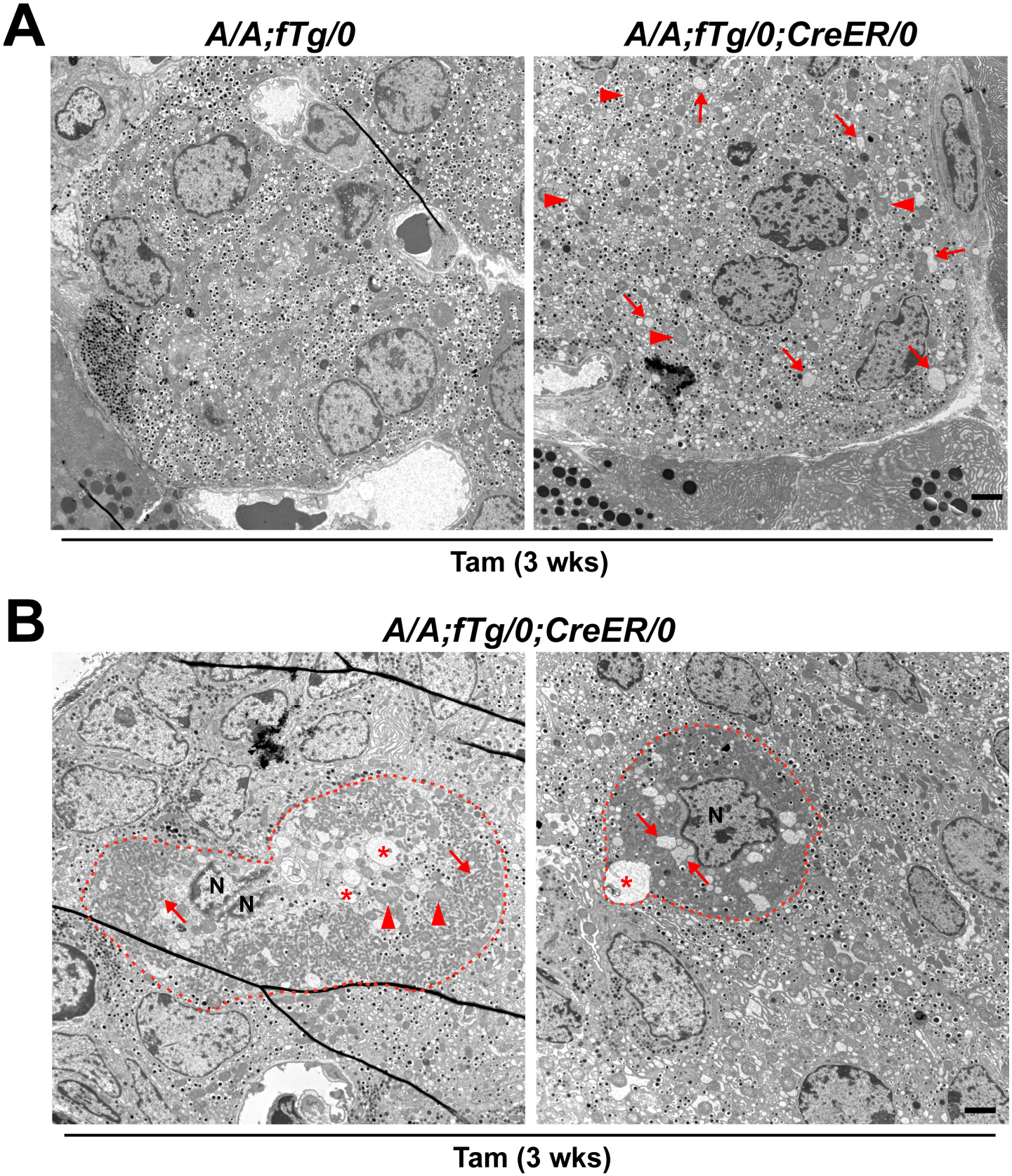

Figure S8C

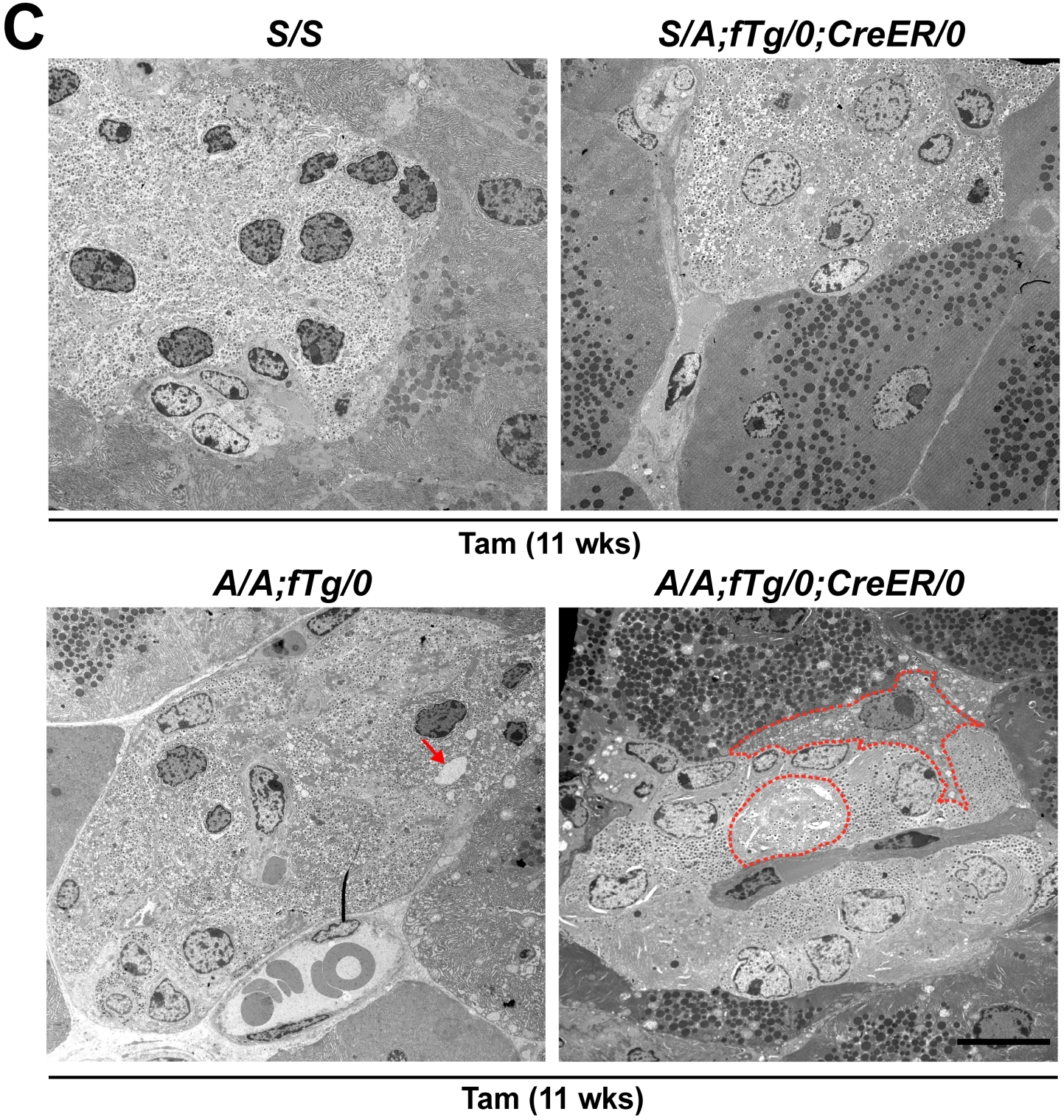

Figure S8D

D

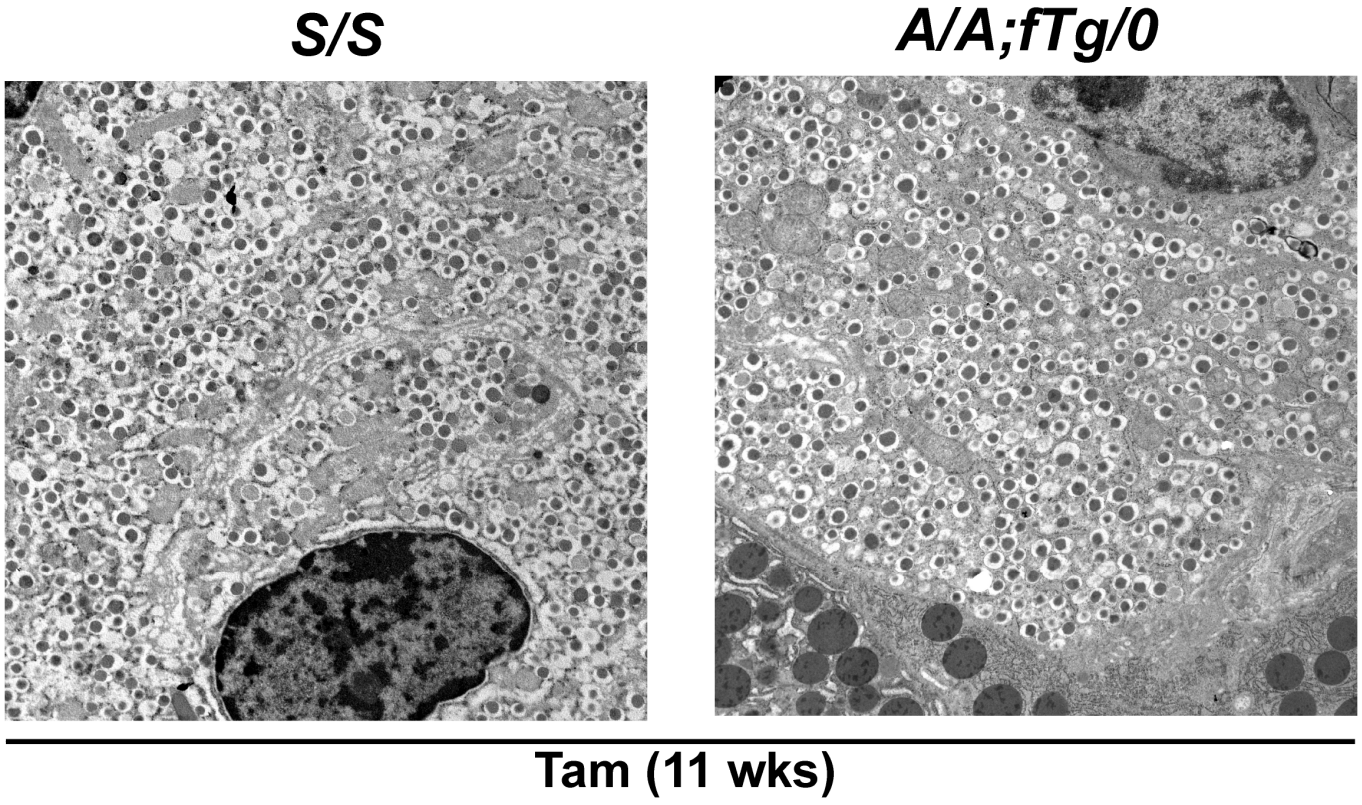

Figure S8. Transmission Electron Microscopy Demonstrates ER Distention, Mitochondrial Swelling, and β Cell Enlargement in Pancreatic Sections from Tamoxifen-Treated *A/A;fTg/0;CreER/0* Mice

Representative transmission electron micrographs are shown from sections of pancreata harvested at 3 (A and B) and 11 (C and D) wks after tamoxifen administration. The dashed lines in the Figure (B) delineate extraordinarily enlarged beta cells. Arrows indicate fragmented or dilated ER, arrowheads demark swollen mitochondria, asterisks indicate abnormal structures of low electron density, and N labels the nuclei of a swollen beta cell. The dashed lines in the fourth panel of Figure (C) delineate infrequent, extremely abnormal beta cells with a reduced number of secretory granules within *A/A;fTg/0;CreER/0* islets. The scale bars represent 2 μm. (A, B, and D) or 10 μm (C).

Figure S9

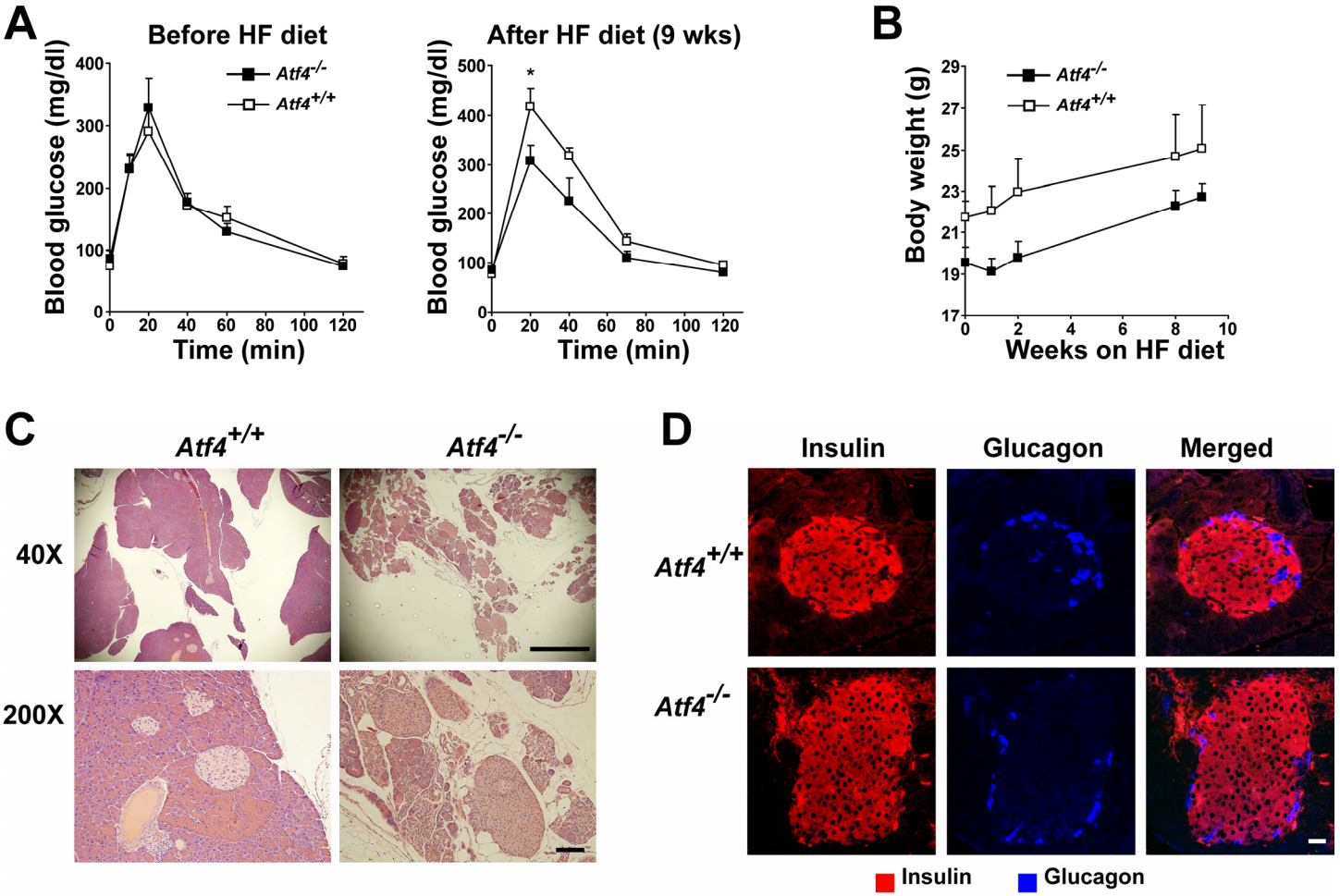
A
Before HF diet
After HF diet (9 wks)
Blood glucose (mg/dl)
Time (min)
Atf4-/-
Atf4+/+
*
B
Body weight (g)
Weeks on HF diet
C
Atf4+/+
Atf4-/-
40X
200X
D
Insulin
Glucagon
Merged
Atf4+/+
Atf4-/-
Insulin
Glucagon
E
Atf4+/+
Atf4-/-
200X
400X

Figure S9. Glucose Homeostasis and Islet Morphology Are Normal in *Atf4*-Null Mice, although Exocrine Tissues Are Apoptotic and Hypoplastic

(A) Glucose tolerance tests were performed before and after 9 wks of 45% high fat diet; n=4 male mice per group.
(B) Body mass was monitored for up to 9 wks of high fat diet.
(C-E) Hematoxylin and eosin staining (C), insulin and glucagon immunolabeling (D), and TUNEL (E) was performed on pancreas tissue sections from male mice (4 month old) fed regular diet. Representative images are shown. The scale bar represents 1000 μM, upper panels, and 100 μm, lower panels (C), 20 μm (D), and 100 μM, upper panels, and 50 μm, lower panels (E).
Data are Mean ± SEM, (A) and (B).

Figure S10

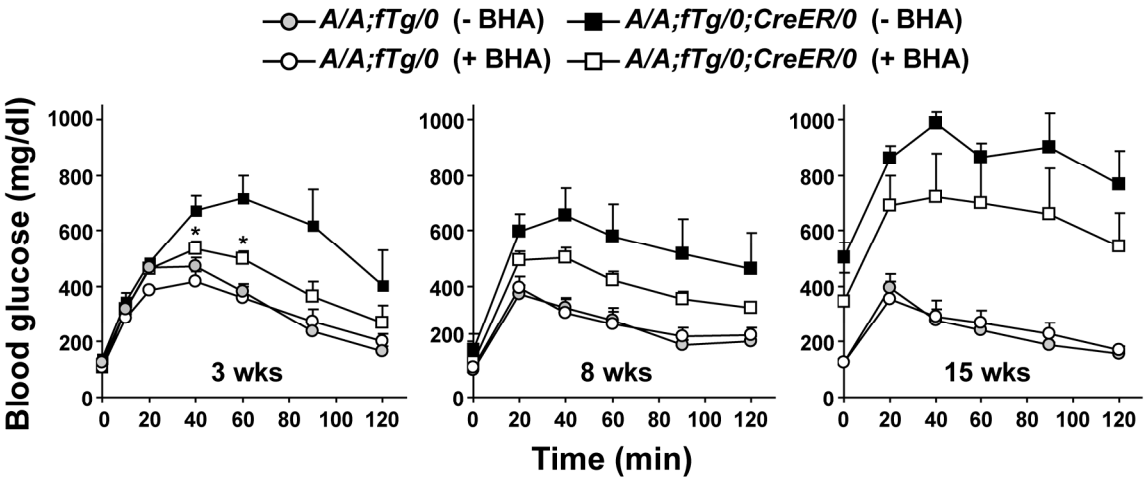

Figure S10. Antioxidant Treatment Improves Glucose Intolerance in *A/A;fTg/0;CreER/0* Mice

Glucose tolerance tests were performed on mice fed chow supplemented with or without BHA for 3-15 wks after Tam treatment. n=5-6 mice per group. Significant differences are defined: *A/A;fTg/0;CreER/0* mice (with BHA) versus *A/A;fTg/0;CreER/0* mice (without BHA), *$P < 0.05. Data are Mean ± SEM.

Quantification of A.U.C. values is shown in main text, Figure 6A.

Supplemental References

Back, S.H., Lee, K., Vink, E., and Kaufman, R.J. (2006). Cytoplasmic IRE1alpha-mediated XBP1 mRNA splicing in the absence of nuclear processing and endoplasmic reticulum stress. J Biol Chem 281, 18691-18706.

Berglund, E.D., Li, C.Y., Poffenberger, G., Ayala, J.E., Fueger, P.T., Willis, S.E., Jewell, M.M., Powers, A.C., and Wasserman, D.H. (2008). Glucose metabolism in vivo in four commonly used inbred mouse strains. Diabetes 57, 1790-1799.

Cano, D.A., Rulifson, I.C., Heiser, P.W., Swigart, L.B., Pelengaris, S., German, M., Evan, G.I., Bluestone, J.A., and Hebrok, M. (2008). Regulated beta-cell regeneration in the adult mouse pancreas. Diabetes 57, 958-966.

Clee, S.M., and Attie, A.D. (2007). The genetic landscape of type 2 diabetes in mice. Endocr Rev 28, 48-83.

D'Alessio, D.A., Verchere, C.B., Kahn, S.E., Hoagland, V., Baskin, D.G., Palmiter, R.D., and Ensinck, J.W. (1994). Pancreatic expression and secretion of human islet amyloid polypeptide in a transgenic mouse. Diabetes 43, 1457-1461.

Hamanaka, R.B., Bennett, B.S., Cullinan, S.B., and Diehl, J.A. (2005). PERK and GCN2 contribute to eIF2alpha phosphorylation and cell cycle arrest after activation of the unfolded protein response pathway. Mol Biol Cell 16, 5493-5501.

Hettmann, T., Barton, K., and Leiden, J.M. (2000). Microphthalmia due to p53-mediated apoptosis of anterior lens epithelial cells in mice lacking the CREB-2 transcription factor. Dev Biol 222, 110-123.

Jiang, H.Y., Wek, S.A., McGrath, B.C., Lu, D., Hai, T., Harding, H.P., Wang, X., Ron, D., Cavener, D.R., and Wek, R.C. (2004). Activating transcription factor 3 is integral to the eukaryotic initiation factor 2 kinase stress response. Mol Cell Biol 24, 1365-1377.

Lee, K., Tirasophon, W., Shen, X., Michalak, M., Prywes, R., Okada, T., Yoshida, H., Mori, K., and Kaufman, R.J. (2002). IRE1-mediated unconventional mRNA splicing and S2P-mediated ATF6 cleavage merge to regulate XBP1 in signaling the unfolded protein response. Genes Dev 16, 452-466.

Mathews, C.E., Bagley, R., and Leiter, E.H. (2004). ALS/Lt: a new type 2 diabetes mouse model associated with low free radical scavenging potential. Diabetes 53 Suppl 1, S125-129.

Nir, T., Melton, D.A., and Dor, Y. (2007). Recovery from diabetes in mice by beta cell regeneration. J Clin Invest 117, 2553-2561.

Onuki, R., Bando, Y., Suyama, E., Katayama, T., Kawasaki, H., Baba, T., Tohyama, M., and Taira, K. (2004). An RNA-dependent protein kinase is involved in tunicamycin-induced apoptosis and Alzheimer's disease. EMBO J 23, 959-968.

Sakaki, K., Wu, J., and Kaufman, R.J. (2008). Protein kinase Ctheta is required for autophagy in response to stress in the endoplasmic reticulum. J Biol Chem 283, 15370-15380.

Scheuner, D., Song, B., McEwen, E., Liu, C., Laybutt, R., Gillespie, P., Saunders, T., Bonner-Weir, S., and Kaufman, R.J. (2001). Translational control is required for the unfolded protein response and in vivo glucose homeostasis. Mol Cell 7, 1165-1176.

Srivastava, S.P., Davies, M.V., and Kaufman, R.J. (1995). Calcium depletion from the endoplasmic reticulum activates the double-stranded RNA-dependent protein kinase (PKR) to inhibit protein synthesis. J Biol Chem 270, 16619-16624.

Zhang, W., Feng, D., Li, Y., Iida, K., McGrath, B., and Cavener, D.R. (2006). PERK EIF2AK3 control of pancreatic beta cell differentiation and proliferation is required for postnatal glucose homeostasis. Cell Metab 4, 491-497.

Zraika, S., Aston-Mourney, K., Laybutt, D.R., Kebede, M., Dunlop, M.E., Proietto, J., and Andrikopoulos, S. (2006). The influence of genetic background on the induction of oxidative stress and impaired insulin secretion in mouse islets. Diabetologia 49, 1254-1263.